Exciton Dynamics in Circular Aggregates: Application to Antenna of Photosynthetic Purple Bacteria

Vladimir I. Novoderezhkin* and Andrei P. Razjivin‡

*Scientific Research Center on Technological Lasers, Russian Academy of Science, Troizk, Moscow Region, 142092, and International Laser Center, Moscow University, Moscow 119899; and ‡A. N. Belozersky Institute of Physico-Chemical Biology, and International Laser Center, Moscow University, Moscow 119899, Russia

ABSTRACT A theoretical model of exciton dynamics in circular molecular aggregates of light-harvesting bacteriochlorophyll of photosynthetic bacteria is proposed. The spectra and anisotropy of photoinduced absorption changes in the femto- and picosecond time domain are under its scope. The excited state of aggregate was treated due to the standard exciton theory, taking into account a pigment inhomogeneity. Dephasing processes via the exciton-phonon interactions were described by means of the Haken-Strobl equation. It was shown that only two exciton levels are dipole-allowed in the case of homogeneous circular aggregate. The pigment inhomogeneity results in the appearance of several weak transitions to higher exciton levels. It was proposed that the minor band (B896) in an absorption spectrum of the B875 complex as well as the similar minor band in spectra of B800–850 complex correspond to electron transition from the ground to the lowest exciton level, whereas the major band corresponds to transition to the higher exciton level. The proposed model shows the subpicosecond decay of anisotropy at the short-wavelength side of absorption band and a high degree of anisotropy at the long-wavelength side, even at high temperatures.

INTRODUCTION

Until now, the dynamics of electronic excitations in the light-harvesting antenna of photosynthetic purple bacteria are not evident. The absence of detailed data on the spacial structure of pigment-protein complexes of purple bacteria hinders the simulation of light absorption, energy transfer, and trapping processes. Recent findings, obtained essentially by ultrafast spectroscopy, result in several different models that in part describe the experimental spectra and kinetic dependencies. However, the theoretical model, which can satisfactory describe all of that data, has not been proposed until now.

The progress made in recent years in the isolation and structure analysis of the light-harvesting antenna complexes of purple bacteria leads to a broader understanding of the structure and function of these complexes (Drews, 1985; Zuber, 1985; Zuber et al., 1987). There are two main types of antenna complexes: the B875 complexes, directly connected with the reaction center (RC); and the B800–850 complexes surrounding the B875 complexes and RC (Thornber et al., 1983). These main complex types may vary slightly for different bacteria (Thornber et al., 1983). The α,β-polypeptide pair with two bound bacteriochlorophyll (BChl) a(b) molecules is the smallest structure unit of the antenna complexes (Zuber, 1985). The primary structure suggests the possible association of the α,β-pairs in the form of cyclic polypeptide complexes: hexamers $\alpha_6\beta_6$ and dodecamers $\alpha_{12}\beta_{12}$ (Zuber et al., 1987; Pearlstein and Zuber, 1985; Zuber and Brunisholz, 1991). Electron microscopy studies also show the circular membrane structures with 100–130 Å diameter, which form two-dimensional hexagonal lattices (Miller, 1982; Engelhard et al., 1983, 1986; Golubok et al., 1992; Meckenstock et al., 1992; Boonstra et al., 1994).

However, these results do not give any information on the location and orientation of BChls in the circular aggregates. Possible BChl arrangements were proposed by Zuber et al. (1987) and Braun and Scherz (1991).

The BChl absorption bands within the near-infrared region are inhomogeneous because of the spectral studies of the light-harvesting antenna of purple bacteria. In the case of the B880 complex from *Rhodospirillum rubrum*, an increase of energy of the exciting pulse was followed by blue-shift of the picosecond absorbance difference spectrum (Borisov et al., 1982; Razjivin et al., 1982; Nuijs et al., 1985; Sundstrom et al., 1986; van Grondelle et al., 1988). The similar results were obtained for the B890 complex from *Chromatium minutissimum* (Danielius et al., 1989) and for the RC-less antenna preparations from *R. rubrum* (Danielius et al., 1986). The blue-shift of the fluorescence emission peak with the excitation energy increase was found at 4 K for *R. rubrum* and *Rhodobacter sphaeroides* chromatophores (Vos et al., 1986) as well as for chromatophores from several *Rhodopseudomonas acidophila* mutants and for membrane fragments from *Rhodopseudomonas viridis* (Deinum et al., 1989).

The inhomogeneity of the B875 absorption band was revealed by derivative spectroscopy (Razjivin et al., 1984), linear and circular dichroism, and fluorescence polarization

Received for publication 31 January 1994 and in final form 16 September 1994.

Address reprint requests to Dr. A. P. Razjivin, Photosynthesis Department, A. N. Belozersky Institute of Physico-Chemical Biology, Moscow State University, Moscow 119899, Russia. Fax: 07-095-939-3181; E-mail: libro@genebee.msu.su.

Abbreviations used: RC, reaction center, B896, absorption band with peak at 896 nm; BChl, bacteriochlorophyll; BChl896, molecule of BChl with absorption peak at 896 nm.

0006-3495/95/03/1089/12 $2.00

(van Grondelle et al., 1988; Kramer et al., 1984) as well as by fluorometry and spectrochronography (spectral dependence of fluorescence lifetime) (Sebban and Moya, 1983; Sebban et al., 1984; Freiberg et al., 1984).

The picosecond kinetics of the induced absorption anisotropy were obtained for the chromatophores from: *R. rubrum* and *Rb. sphaeroides* at 300 K (Sundstrom et al., 1986) and at 77 K (van Grondelle et al., 1987; Hunter et al., 1990); for the isolated B875 complex from *Rb. sphaeroides* at 77 K (Bergstrom et al., 1988); for chromatophores from RC-less mutants *Rb. sphaeroides* at 77 K (Hunter et al., 1990). The two-component kinetics were obtained for the induced absorption changes (for the same polarization of pump and probe pulses). According to Bergstrom et al. (1988), the fast component ($\tau = 15 \pm 5$ ps for the isolated B875 complex) corresponds to energy equilibration between spectrally nonequivalent pigments, and the slow one ($\tau = 600$ ps) corresponds to excitation lifetime in the antenna. In the case of the short-wavelength excitation ($\lambda < 880$ nm), photoinduced absorption changes were characterized by a low anisotropy ($r < 0.1$), but in the case of the long-wavelength excitation ($\lambda > 890$ nm), they were characterized by a high anisotropy ($r = 0.25$). Moreover, a low anisotropy at the short-wavelength side was observed even at the short time intervals (less than 1 ps after excitation), whereas a high anisotropy at the long-wavelength side did not decrease in the picosecond time domain, even at room temperature.

The fast (10–30 ps) component was also obtained in the fluorescence decay for several purple bacteria preparations at 4 and 77 K (Freiberg et al., 1984; Godik et al., 1987; Timpmann et al., 1991; Pullerits and Freiberg, 1991; Godik et al., 1993).

The inhomogeneous broadening of the antenna of purple bacteria was shown (van Grondelle et al., 1992; Visschers et al., 1993; van Mourik et al., 1993; Pullerits et al., 1994). Direct measurements of the inhomogeneous width were carried out for B800–850 and B875 complexes from *Rb. sphaeroides* (Reddy et al., 1991, 1992). The inhomogeneous width for these complexes was found to be equal to 60 and 80 cm^{-1}, respectively. In turn, the homogeneous width for these complexes was equal to 210 and 200 cm^{-1} respectively. Similar results were obtained for the B800–850 complex from *R. acidophila* (Reddy et al., 1993).

Several models were proposed to account for the experimental data listed above. These models may be divided into three groups. The first one includes models based on the assumption that the antenna of purple bacteria contains unknown components (the new spectral forms of bacteriochlorophyll molecules). To the second group may be assigned models that offered to interpret all experimental effects as a result of inhomogeneous broadening of pigment bands. The third group of models is based on the assumption of exciton interactions of the antenna pigment molecules.

Minor spectral form of bacteriochlorophyll

According to the first (Borisov et al., 1982; Razjivin et al., 1982) and now widely accepted interpretation (Sundstrom et al., 1986; van Grondelle et al., 1987; Hunter et al., 1990), the spectral inhomogeneity of the long-wavelength band of the light-harvesting antenna of purple bacteria is due to a minor fraction of bacteriochlorophyll molecules with the absorption peak at a longer wavelength than the peak position of a major part of this pigment molecules ("minor spectral form of bacteriochlorophyll"). The spectral shift between the peaks of minor and major BChls is 10–15 nm. In the case of *R. rubrum* chromatophores at room temperature, according to picosecond absorbance difference spectroscopy the bleaching peak is at 896 nm (Danielius et al., 1984; Sundstrom et al., 1986)).

The short-lived component (10–30 ps) of two-exponent kinetics of induced absorption changes was interpreted by Sundstrom et al. (1986) to be a result of energy transfer from the major pigment molecules (BCh1875) to the minor form molecules (BChl896). The migration of localized excitation over the BChl875 molecules gives the fast (subpicosecond) depolarization (Sundstrom et al., 1986). Then this excitation is transferred to minor form B896, which is presented by the sole molecule BCh1896 in the B875 complex and remains there. Such a model explains a high anisotropy at the long-wavelength side of the fluorescence and induced absorption spectra.

In the RC-less mutant M2192 from *Rb. sphaeroides*, the antenna is an aggregate of the B875 complexes (about 125 BChl molecules per domain (Hunter et al., 1990)). The energy transfer time B875 → B896 increases up to 35 ± 5 ps for such aggregates. The anisotropy at the long-wavelength side ($\lambda > 900$ nm) decreases down to 0.15. According to Hunter et al. (1990), these facts may be explained by the energy migration between B875 complexes.

Unfortunately, the biochemical methods give no evidence for existence of the minor form BChl molecules. Moreover, the antenna model with the long-wavelength minor form has problems connected with interpretation of following facts:

1) The preference localization of excitations within minor form at room temperature, which supposes the potential barrier threefold of the energy gap between these forms (Valkunas et al., 1985);
2) The large value of induced absorption changes per absorbed quantum at bleaching peak of minor form (Abdourakhmanov et al., 1986);
3) The subpicosecond decay of induced absorption anisotropy at the short-wavelength side (Sundstrom et al., 1986; van Grondelle et al., 1987)

Inhomogeneous broadening

According to models of the second group (see above), the B875 band consists of more than two spectral components (Visschers et al., 1993; van Grondelle et al., 1992; Pullerits et al., 1994). Optical nonidentity of pigment-protein complexes in the antenna is the reason of static inhomogeneous broadening of absorption and fluorescence bands (Pullerits and Freiberg, 1991; van Grondelle et al., 1992; Pullerits and Freiberg, 1992; Pullerits et al., 1994).

However, several discrepancies between the inhomogeneous broadening model and experimental data uprise.

First, the direct measurements of homogeneous and inhomogeneous widths for the B875 and B800–850 bands (Reddy et al., 1991, 1992, 1993) show that the inhomogeneous broadening is much less then the overall widths of these bands. So the origin of the minor spectral form cannot be explained by the inhomogeneous broadening.

Second, it is difficult to explain the ultrafast (subpicosecond) induced absorption depolarization at the short-wavelength side of absorption band. According to van Grondelle et al. (1992) and Somsen et al. (1994), such a subpicosecond component is available in a spacially disordered system. However, the speculation that the antenna pigments have a high degree of spacial disorder is in contradiction with the structural data, suggesting a high symmetry of the antenna (C_6-symmetry (Miller, 1982; Engelhard et al., 1983; Engelhard et al., 1986; Golubok et al., 1992; Meckenstock et al., 1992) or C_{12}-symmetry (Boonstra et al., 1994)).

Third, the inhomogeneous broadening unable to give a high anisotropy at the long-wavelength side, especially at high temperatures.

Exciton interactions between BChl molecules in the antenna

There is some speculation in literature that the spectral inhomogeneity of the antenna is due to exciton interactions of the BChl molecules, which case the appearance of several lines in the spectrum, corresponding to exciton levels. The filling of the lowest level leads to the blue-shift of absorption and fluorescence spectra. In several papers (Nuijs et al., 1985; Bergstrom et al., 1988), the exciton hypothesis was claimed to be one of the possible interpretations of the picosecond absorbance difference spectra at low and high excitation energy. However, these authors later gave preference to the other explanations (van Grondelle et al., 1988; Hunter et al., 1990; van Grondelle et al., 1992).

The application of exciton theory to the photosynthetic antenna is associated with some problems.

A theory of molecular excitons has been developed in details only for molecular crystals (Davydov, 1971). The light-harvesting antenna complexes, in contrast to molecular crystals, are finite-sized aggregates of BChl molecules. Such finite aggregates are lacking exciton band and show only discrete exciton levels. The boundary conditions for the finite aggregate may result in the other optical selection rules than those for the infinite crystals. In particular, the higher levels can be dipole-allowed as well as the lowest one. The optical spectra and exciton dynamics calculations for linear, one-dimensional aggregates of finite size were carried out in Aslangul and Kottis (1974, 1976, 1978), Aslangul and Kottis (1978), Rahman et al. (1979), Grad et al. (1988), and Spano et al. (1990). In these papers (excluding the paper of Spano et al., 1990), the exciton dynamics have been described by means of the stochastic Liouville equation (Haken and Strobl, 1967; Reineker, 1982).

To simulate the optical properties of finite aggregates that depend on nonlinear susceptibilities (for example, the excited state absorption), one must to take into account the exciton statistics. Chesnut and Suna (1963) showed that the Frenkel excitons in one-dimensional aggregates (the finite linear chains and finite circular aggregates) exhibit fermion behavior. The excited-state absorption for the linear aggregate has been calculated by Juzeliunas (1988) and Knoester (1993). It was shown that the excited-state absorption spectrum is blue-shifted with respect to the ground-state absorption spectrum.

The concept of exciton interaction in the linear aggregates was used for an interpretation of the induced absorption spectra in chlorosomes from the green photosynthetic bacteria (Lin et al., 1991).

The circular aggregates, unlike the linear ones, have only two dipole-allowed exciton levels with different anisotropies (Novoderezhkin, 1992; Novoderezhkin and Razjivin, 1993a, b; Danielius et al., 1994). In these papers, it was assumed that exciton interactions in circular aggregates are responsible for the shape of absorption and fluorescence spectra of the light-harvesting antenna of purple bacteria. This model is in good agreement with the structural data on polypeptide α,β-pairs association in the form of cyclic structures (Zuber, 1985; Zuber et al., 1987). As follows from the circular aggregate model (Novoderezhkin, 1992; Novoderezhkin and Razjivin, 1993a, b), the minor band in absorption spectra of the B875 and B800–850 complexes corresponds to the transition from the ground to the first (lowest) exciton level, whereas the major band corresponds from the ground to the second exciton level. The other levels are forbidden in the circular aggregates. Notice that this statement is valid only for a homogeneous antenna. The influence of pigment inhomogeneity will be discussed below.

It should be noted that exciton interactions in circular aggregates were treated by Pearlstein and Zuber (1985) and Reddy et al. (1992) for simulations of optical spectra of the light-harvesting complexes of purple bacteria. The special case of circular aggregate with the dipole moments arranged in the aggregate plane was analyzed in both papers. Such a spacial model fails to explain essential optical properties as, for example, the circular dichroism (for coplanar dipoles the CD is equal to zero).

The case of an arbitrary orientation of dipole moments was analyzed by van Metter (1977), Knox and van Metter (1979), and Shepanski and Knox (1981) only for the simplest circular aggregate of three chlorophyll *b* molecules of the chlorophyll *a/b* complex from higher plants. In particular, the CD spectra were calculated (Shepanski and Knox, 1981).

It might be valuable to point out that the pigment inhomogeneity (Timpmann et al., 1991; Pullerits and Freiberg, 1991; Visschers et al., 1993; van Mourik et al., 1993) can influence the exciton states of antenna. However, the inhomogeneous width for B875 complex (80 cm^{-1}; Reddy et al., 1992) is much less than the energetic gap between exciton levels (i.e., the energy gap between B880 and B896 levels), which is equal to 150–200 cm^{-1}. That is why the diagonal disorder due to the pigment inhomogeneity will not destroy

coherent exciton states. In this case, the influence of the diagonal energy disorder Hamiltonian on the exciton eigenstates can be treated perturbatively (Knapp, 1984; Reddy et al., 1992; Knoester, 1993).

The aim of this paper is a theoretical investigation of exciton dynamics in the circular BChl aggregates of the antenna of photosynthetic purple bacteria. The excited states of aggregate are described according to the standard exciton theory excluding the vibronic structure of spectra. The diagonal energy disorder due to a pigment inhomogeneity is treated perturbatively. Dephasing processes arising from the exciton-phonon interactions are taken into account by means of the Haken-Strobl equation.

The theoretical results are used for interpretation of experimental data on the induced absorption anisotropy in the antenna of purple bacteria. These results predict several effects that may take place in the experiments with femtosecond pulses when the coherent excitation of several exciton levels is possible.

THE MODEL

Several electron and tunnel microscopic studies revealed the circular structures in the antenna with the C_6-symmetry (Miller, 1982; Engelhard et al., 1983; Engelhard et al., 1986; Golubok et al., 1992; Meckenstock et al., 1992) or C_{12}-symmetry (Boonstra et al., 1994). So we accept an arrangement of light-harvesting BChls in the form of circular aggregate with the C_N-symmetry, where N is the number of sites, each of which contains m BChl molecules. For example, in the case of the B875 complex-RC with the C_6-symmetry (Miller, 1982; Engelhard et al., 1983; Engelhard et al., 1986; Golubok et al., 1992; Meckenstock et al., 1992), each particle contains the RC and six antenna globules around it in the same plane. Each antenna globule contains four polypeptides and four BChl molecules. For that circular aggregate of BChl molecules $N = 6$, $m = 4$. In the case of the C_{12}-symmetry (Boonstra et al., 1994), one can accept $N = 12$, $m = 2$. In general, an exciton band is splitted on m branches (Davydov components of the exciton band), each containing N levels (Davydov, 1971).

In this paper, we consider the simplest case of one molecule per site ($m = 1$) (Fig. 1). Whole antenna consists of N identical BChl molecules. Each molecule has two electronic states: the ground state and the first excited state.

The Hamiltonian of the electronic excitation can be expressed as (Chesnut and Suna, 1963; Davydov, 1971)

$$\hat{H} = \sum_{n=1}^{N} (\Delta E + \Delta_n) P_n^+ P_n + \sum_{n=1}^{N-1} M (P_n^+ P_{n+1} + P_{n+1}^+ P_n) + M (P_1^+ P_N + P_N^+ P_1), \quad (1)$$

where ΔE is the excitation energy of an isolated molecule; Δ_n describes the energy disorder due to a pigment inhomogeneity; P_n^+, P_n is Pauli creation and destruction operators of the nth molecule; M is the matrix element of excitation transfer between nearest-neighbor molecules (let everywhere below $M < 0$); the interactions with phonon and vibrational modes are neglected.

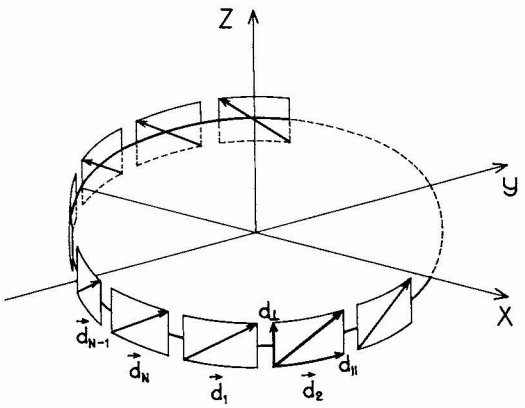

FIGURE 1 The model of light-harvesting antenna. The total number of bacteriochlorophyll molecules in the circle is N; $\vec{d}_n$ is the transition dipole moment of the nth molecule; $\vec{x}$, $\vec{y}$, $\vec{z}$ are the unit vectors of the cartesian coordinate system.

TRANSITION DIPOLE MOMENTS FOR THE HOMOGENEOUS ANTENNA

Diagonalization of the Hamiltonian (Eq. 1) in the case of $\Delta_n = 0$ can be performed by transformation of Pauli operators P_n^+, P_n to the fermion creation and destruction operators b_k^+, b_k (Chesnut and Suna, 1963)

$$H = \sum_k E_k b_k^+ b_k, \qquad E_k = \Delta E + 2M \cos \nu k, \qquad \nu = 2\pi/N \quad (2)$$

$$b_k^+ = N^{-1/2} \sum_{n=1}^{N} e^{-i\nu kn} (-1)^{\sigma_n} P_n^+, \qquad \sigma_n = \sum_{m=1}^{n-1} P_m^+ P_m,$$

where k takes N integer values within the Brillouin zone ($-\pi < k\nu \leq \pi$) for the odd number of excitations in an aggregate (the odd values of σ_{N+1}) and N half-integer values within the same limits for the even number of excitations in an aggregate (the even values of σ_{N+1}).

For example, in the case of even N it will be $k = 0, \pm 1, \pm 2, \cdots, \pm(N-1)/2, N/2$ for one-exciton states and $k = \pm 1/2, \pm 3/2, \cdots \pm(N-1)/2$ for two-exciton states. That is why the level energies and eigenfunctions depend on the quantity of excitations, which distinguish the circular aggregates from linear ones with periodical boundary conditions (Chesnut and Suna, 1963).

The operator of the total transition dipole moment of the aggregate is given by

$$d = \sum_n \vec{d}_n (P_n^+ + P_n)$$
$$\vec{d}_n = d_\parallel \vec{x} \cos \nu n + d_\parallel \vec{y} \sin \nu n + d_\perp \vec{z}, \quad (3)$$

where $\vec{d}_n$ is the transition dipole moment of the nth molecule; $\vec{x}$, $\vec{y}$, $\vec{z}$ are the unit length vectors.

The dipole moments of transitions from the ground state $|g\rangle$ to the one-exciton states $|k\rangle = b_k^+ |g\rangle$

$$\langle k|\hat{d}|g\rangle = N^{1/2}(d_\parallel/2\,(\vec{x} \pm i\vec{y})\delta_{k,\pm 1} + d_\perp \vec{z}\delta_{k,0}) \quad (4)$$

are nonzero only for the two lowest exciton components,

$k = 0$ and $k = \pm 1$. The lowest level, $k = 0$, corresponds to absorption of an incident electromagnetic wave $\vec{E} = \vec{e}E \exp(i\omega t)$ with the linear polarization ($\vec{e} = \vec{z}$) and has high absorption anisotropy. The twofold degenerated level, $k = \pm 1$, corresponds to absorption of the circularly polarized light ($\vec{e} = (\vec{x} \pm i\vec{y})/\sqrt{2}$) and has low absorption anisotropy. Notice that in Eq. 4 axis $\vec{x}$ is aligned with the projection of $\vec{E}$ on the $\vec{x}O\vec{y}$, and the result is independent of orientation of this projection with respect to $\vec{d}_n$. The energy, corresponding to transitions between states $|g\rangle$ and $|k\rangle$ is equal to E_k (see Eq. 2).

The dipole moments of transitions from the one-exciton state $|k\rangle$ to the two-exciton states $|k_1k_2\rangle = b^+_{k1}b^+_{k2}|g\rangle$ are equal to

$$\langle k_2k_1|\hat{d}|k\rangle = N^{1/2}(d_\parallel/2(\vec{x} \pm i\vec{y})F_{\pm 1}\delta_{k1+k2,k\pm 1} + d_\perp \vec{z}F_0\delta_{k1+k2,k}) \quad (5)$$

$$F_\epsilon = \frac{i\nu}{2\pi}\left[\mathrm{ctg}\left(\frac{(k_2-\epsilon)\nu}{2}\right) - \mathrm{ctg}\left(\frac{(k_1-\epsilon)\nu}{2}\right)\right], \quad \epsilon = 0, \pm 1.$$

In Eq. 5 k_1 and k_2 take the half-integer values, whereas k has the integer values. The axis $\vec{x}$ is aligned with the projection of $\vec{E}$ on the $\vec{x}O\vec{y}$ plane, where $\vec{E}$ belongs to light pulse that creates the state $|k\rangle$. The k_1, k_2, and k values are determined to a precision of $\nu/2\pi$, i.e., $k \pm N = k$. One has to take it in account when Kronneker's δ-symbol in Eq. 5 is calculated. The transition energy between levels $|k\rangle$ and $|k_1k_2\rangle$ is equal to $E_{k1,k2} = E_{k1} + E_{k2} - E_k$.

CONSIDERATION OF PIGMENT INHOMOGENEITY

We have found the eigenstates and eigenfunctions for a homogeneous circular aggregate in the previous section. Now we need to determine the first-order correction due to diagonal energy disorder.

For $\Delta_n \neq 0$ in the zero order approximation of perturbation theory, each twofold degenerative level $|\pm k\rangle$ with the energy E_k will split into two sublevels $|k\rangle_\pm$ with the energies $E^\pm_k$, where $k = 1, 2, \cdots (N/2 - 1)$:

$$|k\rangle_\pm = 2^{-1/2}(|k\rangle \pm e^{-i\phi}|-k\rangle)$$

$$E^\pm_k = E_k + V_{k,k} \pm |V_{k,-k}|; \qquad V_{k,-k} = |V_{k,-k}|\, e^{i\phi} \quad (6)$$

$$V_{k1,k2} = \langle k_1|\Delta_n P^+_n P_n|k_2\rangle.$$

In the first-order approximation of perturbation theory, one can obtain for the levels $k = 1, 2, \cdots (N/2 - 1)$:

$$|k\rangle'_\pm = |k\rangle_\pm + \sum_{k'=1}^{N/2-1}\frac{V^\pm_{k',k}}{E_k - E_{k'}}|k'\rangle_\pm + \sum_{k'=0,N/2} 2^{-1/2}\frac{V^\pm_{k',k}}{E_k - E_{k'}}|k'\rangle \quad (7)$$

$$V^\pm_{k',k} = V_{k',k} \pm e^{-i\phi}V_{k',-k}.$$

For the nondegenerative levels $k = 0$, $N/2$ it will be

$$|k\rangle' = |k\rangle + \sum_{k'}\frac{V_{k',k}}{E_k - E_{k'}}|k'\rangle \qquad E'_k = E_k + V_{k,k} \quad (8)$$

(in all sums, the term with $k' = k$ is omitted).

The calculations of transition dipole moments using Eqs. 6–8 show that in the case of diagonal disorder the transitions to higher exciton levels are optically allowed. The corresponding transition dipole moments are the linear combinations of dipole moments given by Eq. 4 with coefficients depending on the $V_{k1,k2}$ values. This results in some smoothing of the wavelength anisotropy dependence within the line. The polarization at the long-wavelength side becomes lower and, at the short-wavelength side, some nonpolarized absorption in the form of a broad wing appears. The level shift being averaged over all aggregates of the antenna gives some broadening of each exciton component.

DENSITY MATRIX EQUATION

The excitation dynamics in an aggregate for $t > 0$ are described by the density matrix:

$$\rho_{k',k''} = \langle k'|\hat{\rho}|k''\rangle \quad (9)$$

We assume that the aggregate is excited at $t = 0$ by laser pulse with the duration τ. The time dependence of density matrix for $t > 0$ may be obtained using the Haken-Strobl equation. In the delocalized basis (Eq. 9), these equations can be written as (Reineker, 1982)

$$\frac{d}{dt}\rho_{k+q,k} = \sum_{k'}\left(\frac{2\gamma_0}{N}\right)(\rho_{k'+q,k'} - \rho_{k+q,k}) - 2iJ(E_{k+q} - E_k)\rho_{k+q,k} \quad (10)$$

$$\frac{d}{dt}\rho_{kk} = \sum_{k'}\left(\frac{2\gamma_0}{N}\right)(\rho_{k'k'} - \rho_{kk}),$$

where $J = M/h$; γ_0 is the phenomenological parameter that describes the dephasing processes due to local fluctuations. In Eq. 10 we neglect parameters γ_{n-m}, which describe the influence of nonlocal fluctuations in the Haken-Strobl equation, assuming $\gamma_{n-m} \ll \gamma_0$ for high temperatures (Reineker, 1982). We also neglect the radiation and nonradiation losses, which have no influence on the fast dephasing processes.

The equations for the diagonal elements have the following solution:

$$\rho_{kk}(t) = (1/N)(1 - e^{-2\gamma_0 t}) + \rho_{kk}(0)e^{-2\gamma_0 t}. \quad (11)$$

The uniform occupation of all exciton levels takes place for $t \to \infty$. Thus, the model is valid only for sufficiently high temperatures when k_BT exceeds $|2M|$, where k_B is the Boltzmann factor and T is the absolute temperature.

The solution of equations for the nondiagonal elements depends on (*i*), a relationship between parameters γ_0 and $|J|$, which characterize the homogeneous linewidth and exciton splitting values and (ii) the initial conditions

determined by an excitation pulse polarization and a ratio between τ, $1/\gamma_0$ and $1/|J|$. The $1/|J|$ value is within tens of femtoseconds as estimated from the energetic gap between the B896 and B880 absorption components. The $1/\gamma_0$ value is not known exactly. According to a theoretical estimation, it is in the range from 10 fs to 1 ps (Pearlstein, 1982).

If the solution of density matrix equations is known, then the kinetics of induced absorption changes and decay of induced absorption anisotropy can be calculated with Eqs. A1–A7 given in Appendix A.

ANALYTICAL SOLUTIONS FOR THE SIMPLEST CIRCULAR AGGREGATE ($N = 3$)

Let us analyze the kinetics of induced absorption anisotropy for the simplest circular aggregate (the trimer) as an example of this theoretical model application. Notice that a similar model of exciton interactions in the trimer was proposed by Knox and van Metter (1979) and Shepanski and Knox (1981) for the light-harvesting chlorophyll *a/b* complex from higher plants. Polarization of the steady-state fluorescence emission spectrum and the circular dichroism spectrum was calculated. Unlike these authors, we will analyze the picosecond kinetics of induced absorption anisotropy. In this case, one must take into account both the transition to one-exciton states and the transitions to higher two-exciton levels. For simplicity, we will restrict the analysis to the case of a homogeneous trimer. Notice that all of the following results are applicable to the chlorophyll *b* trimer of light-harvesting chlorophyll *a/b* complexes from higher plants.

The trimer has three one-exciton levels. All of these levels are dipole-allowed. It has three two-exciton levels as well. The scheme of levels for $M < 0$ and spectral line positions, corresponding to transitions between these levels, is shown in Fig. 2. It is convenient to characterize the position of spectral lines by the dimensionless parameter α, which is equal to the energy measured from ΔE and normalized on $|M|$.

Before the discussion of the case $N = 3$, several common notes have to be mentioned concerning with influence of N value on a difference spectrum shape and a character of exciton dynamics in the circular aggregates.

As seen in Fig. 2, the excited-state absorption spectrum is blue-shifted with respect to the ground-state absorption spectrum for $N = 3$. This effect is less pronounced for the trimer than for larger aggregates, whose excited-state absorption spectra contain more short-wavelength lines corresponding to the transitions to higher two-exciton states. The trimer lacks these two-exciton states.

The increase of N value is followed by the appearance of new short-wavelength lines (the transitions to higher two-exciton levels) as well as by the change in position of the lowest two-exciton levels relative to the levels $|0\rangle$ and $|\pm1\rangle$. For example, the line of transition $|\pm1\rangle \rightarrow |\pm\frac{1}{2}, \pm\frac{3}{2}\rangle$ is red-shifted relative to the line of transition $|g\rangle \rightarrow |\pm1\rangle$ for $N = 3$, coincides with it for $N = 4$, and is blue-shifted for $N \geq 5$.

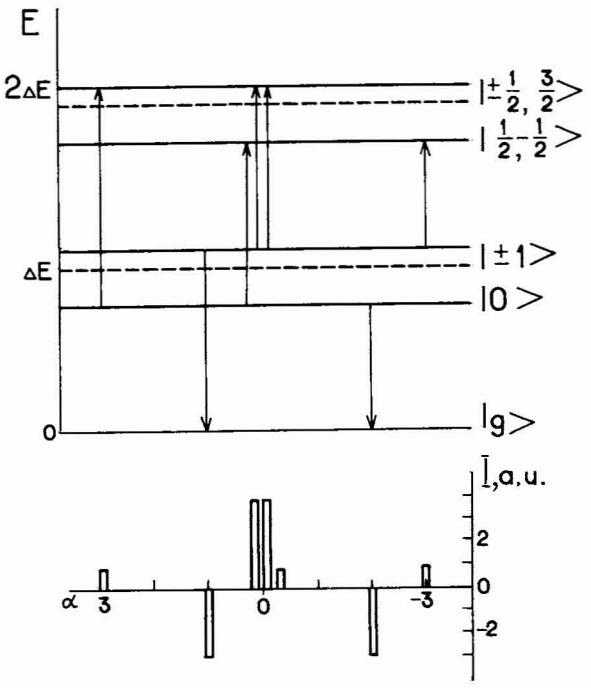

FIGURE 2 The scheme of excitonic levels for the trimer ($N = 3$, $\kappa^2 = 1$) and relative intensities of spectral lines for transitions from one-exciton states.

As a result, the difference spectra of large circular aggregates have a negative branch at the long-wavelength side (the absorption from the ground state) and a broad positive branch (the absorption from excited states) at the short-wavelength side. The difference spectrum shape for arbitrary N was analyzed in our previous papers (Novoderezhkin and Razjivin, 1993a, Danielius et al., 1994).

Let us discuss analytical expressions of the induced absorption anisotropy for $N = 3$ in the broad-band and narrow-band pump and probe limits. The induced absorption anisotropies were calculated by averaging over all possible orientations of $\vec{e}_p$ (see Appendix A) in the $\vec{x}O\vec{y}$ and $\vec{x}O\vec{z}$ planes.

Broad-band pump and probe ($N = 3$, $\vec{x}O\vec{y}$ plane)

In the case of broad-band pump and probe ($1/\tau \gg |J|, \gamma_0$), when the coherent interaction with all exciton levels is possible, the anisotropy degree for the vector $\vec{e}_p$ lying in the $\vec{x}O\vec{y}$ plane is equal to

$$p(\vec{x}O\vec{y}) = \tfrac{1}{2}e^{-4/3\gamma_0 t}(1 + (4\gamma_0/9J)\sin 3Jt); \qquad \gamma_0 \ll |J|$$

$$p(\vec{x}O\vec{y}) = \tfrac{1}{2}(3e^{-3Ft} - e^{-2\gamma_0 t}); \qquad \gamma_0 \gg |J| \tag{12}$$

$$F = J^2/\gamma_0;$$

Only elements $\rho_{1,1}$, $\rho_{-1,-1}$, and $\rho_{-1,1}$ are nonzero at $t = 0$ because of the coherent interaction of excitation pulse with the $|g\rangle \rightarrow |\pm1\rangle$ transitions. An interference of the states

$|1\rangle$ and $|-1\rangle$ results in the excitation density distribution $\cos^2 2\pi(n - m_0)/N$, where n is the number of molecules in aggregate, m_0 depends on an orientation of $\vec{e}_p$ ($0 \le m_0 < N$). Thus, the induced absorption anisotropy at $t = 0$ is high.

$\gamma_0 \ll |J|$

The anisotropy degree exponentially falls to zero with the time constant $(4/3\gamma_0)^{-1}$. This decay is modulated by the low amplitude sinusoidal function. The modulation arises from the coherence between the states $|\pm 1\rangle$ and $|0\rangle$ (the elements $\rho_{1,0}$ and $\rho_{-1,0}$) for $t > 0$. The amplitude of these oscillations is proportional to $\rho_{1,0} \sim \gamma_0/|J|$.

$\gamma_0 \gg |J|$

The equilibration of $\rho_{-1,1}$ and $\rho_{1,0}$ ($\rho_{-1,0}$) takes place with the time constant $(2\gamma_0)^{-1}$. This results in the equilibration of exciton level populations $\rho_{1,1}$ ($\rho_{-1,-1}$) and $\rho_{0,0}$ with the same time constant, but the spacial modulation of excitation density is still retained. Later, $\rho_{-1,1}$ and $\rho_{1,0}$ ($\rho_{-1,0}$) decay with the time constant $(3F)^{-1}$, where F is the Forster rate of the intermolecular energy transfer. This decay corresponds to the spatial equilibration of excitation density caused by the Forster energy migration via molecules within aggregate. The similar effect in the case of dimer and its influence on the fluorescence depolarization of dimer under broad-band laser pulse excitation was analyzed by Rahman et al. (1979) and Knox and Gulen (1993).

Broad-band pump and probe ($N = 3$, $\vec{x}O\vec{z}$ plane)

The anisotropy degree for the vector $\vec{e}_p$ lying in the $\vec{x}O\vec{z}$ plane is equal to

$$p(\vec{x}O\vec{z}) = \frac{1}{2}\frac{(1 - e^{-2\gamma_0 t})A_- + e^{-2\gamma_0 t}B_- - C_-(t) - D_-}{(1 - e^{2\gamma_0 t})A_+ + e^{-2\gamma_0 t}B_+ - C_+(t) - D_+};$$

$$A_\pm = \tfrac{1}{9}(\kappa^2 \pm 2)(5\kappa^2 \pm 7);$$

$$B_\pm = \kappa^4 \pm 5/3\kappa^2 + \tfrac{4}{3};$$

$$D_\pm = (\kappa^2 \pm 2)^2; \qquad \kappa = 2d_\perp/d_\parallel; \tag{13}$$

$$C_+ = \tfrac{2}{3}(3\,e^{-3Ft} - e^{-2\gamma_0 t});$$

$$C_- = C_+ + 2\kappa\,(e^{-3Ft} + e^{-2\gamma_0 t}); \qquad \gamma_0 \gg |J|;$$

$$C_+ = \tfrac{4}{3}e^{-4/3\gamma_0 t};$$

$$C_- = C_+(1 + 3\kappa\cos 3Jt); \qquad \gamma_0 \ll |J|;$$

In general, all elements of the density matrix are nonzero at the initial time moment.

$\gamma_0 \ll |J|$

The value $\rho_{1,0}$ cannot be treated as a small quantity. In this case, the time dependence of anisotropy degree comprises an exponential decay curve with large amplitude oscillations.

$\gamma_0 \gg |J|$

The anisotropy degree approaches some limiting value that is dependent on κ.

Narrow-band pump and probe ($N = 3$, $\vec{x}O\vec{y}$ plane)

In the case of narrow-band pump and probe ($\gamma_0 \ll 1/\tau \ll |J|$), the expression for anisotropy degree takes form

$$p(\vec{x}O\vec{y}) = \frac{e^{-4/3\gamma_0 t}E}{(1 - e^{-2\gamma_0 t})G - e^{-2\gamma_0 t}H - I}. \tag{14}$$

The coefficients in Eq. 14 are the functions of pump and probe pulse frequencies (see Appendix B).

An important distinctive property of the circular aggregate is a presence of twofold degenerated, dipole-allowed level $|\pm 1\rangle$. In the linear aggregate, all exciton levels are nondegenerated. Therefore, the coherent excitation of at least two exciton levels requires broad-band pump pulses. In the circular aggregate, the coherent excitation of two exciton levels, corresponding to an additional anisotropy in the $\vec{x}O\vec{y}$ plane, can be induced by a narrow-band pulse. This pulse can excite the levels $|1\rangle$ and $|-1\rangle$, which have the same transition energy. The anisotropy degree tends to zero for $t \gg \gamma_0^{-1}$.

Narrow-band pump and probe ($N = 3$, $\vec{x}O\vec{z}$ plane)

The expression for anisotropy degree takes form

$$p(\vec{x}\,O\vec{z}) = \frac{1}{2}\frac{(1 - e^{-2\gamma_0 t})A_- + e^{-2\gamma_0 t}B_- + e^{-4/3\gamma_0 t}C_- - D_-}{(1 - e^{-2\gamma_0 t})A_+ + e^{-2\gamma_0 t}B_+ + e^{-4/3\gamma_0 t}C_+ - D_+}. \tag{15}$$

The coefficients in Eq. 15 are the functions of pump and probe pulse frequencies (see Appendix B).

If the vector $\vec{e}_p$ is oriented in the $\vec{x}O\vec{z}$, plane then an anisotropy degree will not decrease to zero at infinite time, unlike the case when the vector $\vec{e}_p$ is parallel to the $\vec{x}O\vec{y}$ plane. The spectral dependence of anisotropy degree is shown in Fig. 3 for the narrow-band limit, when $t \gg \gamma_0^{-1}$ and frequencies of pump and probe pulses are the same ($f_p \equiv f$, see Appendix A). The Gaussian shape was assumed for the f function. The high anisotropy degree ($p = 0, 5$) is seen from Fig. 3 at the short-wavelength side (at $\alpha > 1$). This curve $p(\alpha)$ has a break at the point, where the $\Delta A_\parallel + \Delta A_\perp$ value is equal to zero. The anisotropy degree decreases between points $\alpha = -2$ and $\alpha = 1$ and increases at the long-wavelength side (in the vicinity of the point $\alpha = -3$). As a result, the anisotropy degree is high ($p = 0.5$) for all components of the difference spectrum.

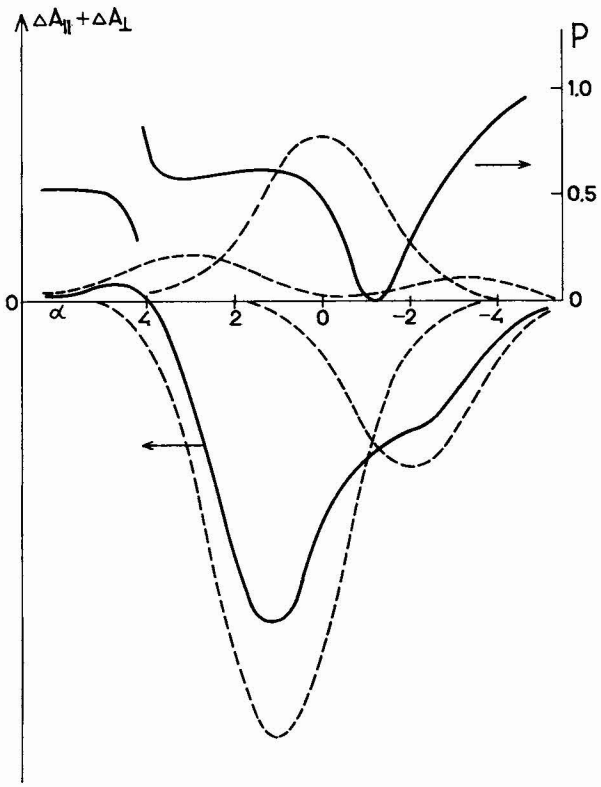

FIGURE 3 The dependence of anisotropy degree on the normalized frequency of pump pulse in the narrow-band limit for $t \gg \gamma_0^{-1}$ and $N = 3$. The frequencies of pump and probe pulses are the same; the vector $\vec{e}_p$ is oriented in the $\vec{x}O\vec{z}$ plane. Contributions of the individual excitonic components (under the assumption of the Gaussian line shape with $d = 1$, where d is the half-width at $1/e$ level, and $\kappa^2 = 2/3$) are shown by dashed lines. The overall $\Delta A_\parallel + \Delta A_\perp$ spectrum is shown by a solid line.

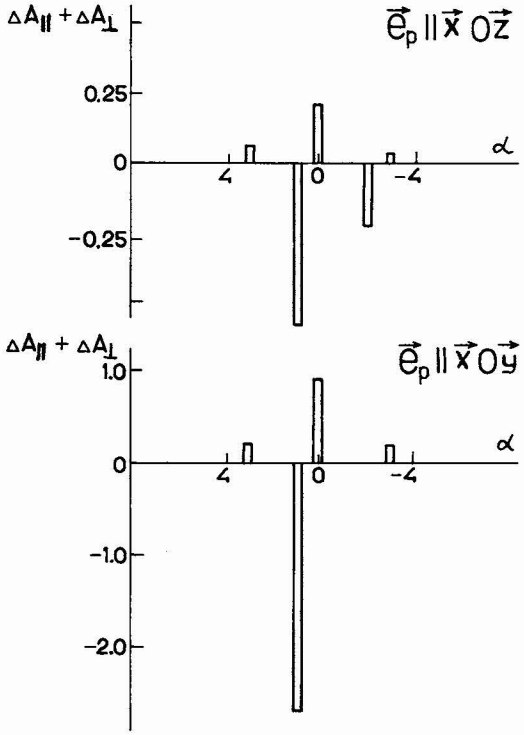

FIGURE 4 The intensities of spectral components of $\Delta A_\parallel + \Delta A_\perp$ spectrum with a low ($\vec{e}_p$ is oriented in the $\vec{x}O\vec{y}$ plane) and a high ($\vec{e}_p$ is oriented in the $\vec{x}O\vec{z}$ plane) anisotropy in the narrow-band limit for $t \gg \gamma_0^{-1}$ and $N = 3$ are shown. The frequencies of pump and probe pulses are the same. The magnitude of each component per absorbed quantum is normalized on $(3/4\ d_\parallel^2)^2$.

Narrow-band pump and probe ($N = 3$, $\vec{x}O\vec{y}$, and $\vec{x}O\vec{z}$ planes)

As shown above, the components of the difference spectrum corresponding to the orientation of $\vec{e}_p$ in the $\vec{x}O\vec{y}$ or $\vec{x}O\vec{z}$ planes are characterized by low ($p = 0$) or high ($p = 0.5$) anisotropy degree at $t \gg \gamma_0^{-1}$ and $f_p \equiv f$ (the same conditions as in one-color, pump-probe experiments (Bergstrom et al., 1988)). The intensity of spectral components of the $\Delta A_\parallel + \Delta A_\perp$ spectrum for these two cases are shown is Fig. 4, where the magnitude of each component per absorbed quantum is normalized on $(3/4\ d_\parallel^2)^2$. The high anisotropy and the low anisotropy components are overlapped for all lines except the line corresponding to $\alpha = -2$. That is why the resulting anisotropy is low within all spectrum with the exception of the long-wavelength wing of absorption band. Here a non-compensated, high anisotropy component is presented, corresponding to the bleaching line with $\alpha = -2$ (the lowest exciton level $|0\rangle$). This component is so called the "minor spectral form."

STEADY-STATE LIMIT (ARBITRARY N)

In the previous section, we studied the special case of $N = 3$ in the high temperature limit ($\rho_{k'k''}(t \to \infty) = \delta_{k'k''}/N$) to obtain the analytical solution for anisotropy kinetics. This simple example allows to illustrate some essential physical properties of exciton dynamics in a circular aggregate. In the more realistic case ($N = 12$ or 24; a finite temperature), the analytical solution may be obtained only for the steady-state limit.

In the steady-state limit, the density matrix elements $\rho_{k'k''}(t)$ in Eqs. A5 and A1 must be replaced by $\delta_{k'k''}\exp(-E_{k'}/k_BT)$. Using Eqs. A1–A7, we can now calculate the steady-state anisotropy for arbitrary temperature and arbitrary N.

To compare the theory with the experimental data (the steady-state anisotropy for *Rb. sphaeroides* and *R. rubrum* chromatophores at 77 K (van Grondelle et al., 1987) and for isolated B875 complexes from *Rb. sphaeroides* at 77 K (Bergstrom et al., 1988), we calculated the anisotropy defined as $r = (\Delta A_\parallel - \Delta A_\perp)/(\Delta A_\parallel + 2\Delta A_\perp)$ or $r = 2p/(3 - p)$ in the narrow-band pump-probe limit. The induced absorption anisotropies were calculated by averaging over all possible orientations of the $\vec{e}_p$. We also assume that $f_p \equiv f$; $f(\alpha) = \exp(-\alpha^2/d^2)$; $d = E_1 - E_0$; $T = 77$ K; E_1 and E_0 correspond to 890 and 900 nm, respectively (van Dorssen et al., 1988); $\kappa^2 = 1$; $N = 24$; $\Delta_n \equiv 0$ (the homogeneous antenna).

The calculated anisotropy $r(\lambda)$ is shown in Fig. 5. The low anisotropy ($r = 0.05$–0.08) is seen in Fig. 5 at the

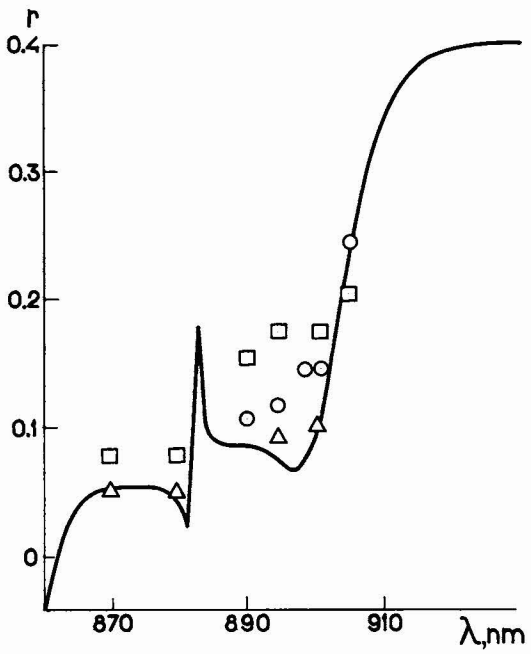

FIGURE 5 The steady-state anisotropy calculated for $N = 24$ and $\kappa^2 = 1$ (——) and measured at 77 K for *Rb. sphaeroides* chromatophores (van Grondelle et al., 1987) (*circles*); *R. rubrum* chromatophores (van Grondelle et al., 1987) (*triangles*); isolated B875 complexes from *Rb. sphaeroides* (Bergstrom et al., 1988) (*squares*).

short-wavelength side ($\lambda < 880$ nm). The curve $r(\lambda)$ has a break at the point, where the $\Delta A_{\parallel} + 2\Delta A_{\perp}$ value is equal to zero. The anisotropy degree is higher within the 885–900 nm range and increases rapidly at the long-wavelength side ($\lambda > 900$ nm). According to our calculations (data not shown), the anisotropy does not depend on N for large aggregates ($N > 6$).

Our calculations are in good agreement with experimental results (see Fig. 5). To obtain a better quantitative fit, one must attempt to take into account the diagonal energy disorder and the vibronic structure of absorption spectrum (Danielius et al., 1994).

In conclusion, we state that the presented model offers a comprehensive explanation of the depolarization kinetics and steady-state values of induced absorption anisotropy obtained in picosecond experiments (Sundstrom et al., 1986; van Grondelle et al., 1987; Bergstrom et al., 1988; Hunter et al., 1990). From our point of view, the subpicosecond depolarization of induced absorption changes at the short-wavelength side is due to the dephasing of exciton states $|1\rangle$ and $|-1\rangle$, whereas the long-lived high anisotropy degree at the long-wavelength side corresponds to high population probability of the lowest exciton level $|0\rangle$ even at room temperature.

DISCUSSION

All exciton processes in the light-harvesting antenna may be subdivided into several groups according to the characteristic time range:1) linear losses (spontaneous radiative and non-radiative processes) with the total time constant around 600 ps (Sebban et al., 1984; Bergstrom et al., 1988);2) excitation quenching by opened and closed RCs with the time constants about 200 and 60 ps (Freiberg et al., 1984; Abdourakhmanov et al., 1986; Sundstrom et al., 1986);3) relaxation processes due to the interaction of excited molecules with microenvironment (protein matrix) with time constants of tens of picoseconds (Danielius et al., 1992, 1994) (it may result in the dynamic red-shift in monocentral isolated objects);4) energy migration between the neighbor circular aggregates in the antenna with the time constants of 10–30 ps at room temperature (according to our calculations) or 5–10 ps at low temperature (Reddy et al., 1992) and our calculations) (it may result in the dynamic red-shift in multicentral objects).5) exciton relaxation from higher exciton levels at low temperatures in subpicosecond time domain (Reddy et al., 1992) (it may results in the ultrafast red-shifts);

The kinetics of induced absorption anisotropy reflect the subpicosecond exciton relaxation and some 10–30 ps relaxation process at time interval $t < 60$ ps.

The subpicosecond anisotropy decay at the short-wavelength side of absorption band along with the maintenance of a high degree of anisotropy at the long-wavelength side of band even at high temperatures can be explained by a dephasing process of exciton states of circular aggregates in photosynthetic light-harvesting antenna. The relaxation processes of exciton interaction with microenvironment are significantly slower than the processes of population equilibration of exciton levels and cannot determine polarization effects.

Danielius et al. (1992) showed that the energy exchange between vibronically excited BChl molecules and protein matrix in the *R. rubrum* chromatophores has the a constant of approximately 20–30 ps. Components with the same time constants (10–30 ps) were found in the picosecond time-resolved fluorescence emission (Timpmann et al., 1991) and difference absorption spectra (Sundstrom et al., 1986; Bergstrom et al., 1988) of several purple bacteria. Danielius et al. (1994) assumed the existence of long-living vibronic excitations due to the interaction of pigment electronic excitations with pseudo-localized librational modes. These librational modes relax slowly through the nonelastic interactions with protein matrix phonons. Notice that the librational modes also have lifetimes on the order of 30 ps in linear molecular aggregates (de Boer et al., 1987).

The vibronic relaxation process with the a constant of 10–30 ps in the antenna can influence the kinetics of fluorescence and induced absorption of monocentral objects consisting of one RC and a core antenna (the B890 complex from *C. minutissimum* (Freiberg et al., 1988) and the B875 complex form *Rb. sphaeroides* (Bergstrom et al., 1988). The chromatophores (multicentral objects) have additional reason for such a 10–30 ps component connected with the energy migration between neighbor antenna circular aggregates ((Reddy et al., 1992) and our calculations).

The results being obtained show that the model of light-harvesting antenna of purple bacteria as a circular aggregate

of BChl molecules allows us to describe experimental data on anisotropy of induced absorption at the quantitative level.

One may propose the other model capable of describing the steady-state anisotropy. According to this model, the light-harvesting antenna consists of several weakly interacting BChl dimers arranged in a circle. Their dipole moments for transition to the lowest exciton level are oriented parallel to the $\vec{z}$ axis as well as the dipole moments for transitions to high level are circular-degenerated in the $\vec{x}O\vec{y}$ plane. However, first, such a dimer model gives the difference spectrum without a blue-shifted positive branch. Second, the dimer model fails to explain a high value of bleaching at the long-wavelength side (at the minor form peak) per absorbed quantum (Abdourakhmanov et al., 1986). This large value of absorption changes per quantum is one of most characteristic features for the circular aggregate of strongly interacted BChl molecules (Chesnut and Suna, 1963).

Let us discuss the approximations that form a basis of the proposed antenna model and exciton dynamics description.

1. In this paper, we analyze the simplest circular aggregate with a one molecule per site ($m = 1$). In general, it is necessary to assume $N = 6, m = 4$ for the B875 complex, which consists of six globules with four BChl molecules in each. In this case, exciton band will be splitted to four branches (Davydov, 1971). All results for $m = 1$ obtained above will be valid for the lowest branch. That is why our model is acceptable for exciton dynamic description at the long-wavelength part of spectra. The extension of the obtained results in the case $m = 4$ is not difficult, but needs some information on the mutual BChl molecule arrangement in globules.
2. The other important assumption is connected with a form of density matrix equations. According to Eq. 10, the excitation transition rate from the k to k' level is equal to the back transition rate. For finite temperature, the ratio of direct and back transitions has to be proportional to Boltzmann factor. Corresponding generalization of these equations is straightforward (Rahman et al., 1979), but its solution will be even more complicated.
3. In our model, we use the Haken-Strobl equation, which accounts for exciton-phonon interaction in the form of δ-correlated fluctuations. Further generalization of the supposed model can be related to the microscopic quantum treatment of exciton-phonon interaction.
4. The interaction of pigment electronic excitations with pseudo-localized (or localized) modes results in the appearance of several levels on the energy diagram corresponding to vibronic sublevels of the ground level $|g)$, one-exciton levels $|k)$, two-exciton levels $|k', k'')$, and so on. An advanced theory of exciton dynamics has to take into account the vibronic structure of exciton levels in a course of approach of Danielius et al. (1994).

The research described in this publication was made possible in part by Grant No. MKG000 from the International Science Foundation and Grant No. 94-04-12779 of the Russian Foundation for Basic Research.

APPENDIX A

Let us denote the probability of light quantum absorption from the ground state by $A^{(1)}_{(g)}$. The absorption of second quantum as well as the induced emission may take place under interaction of the probe pulse with excited aggregate. Corresponding probabilities are denoted by $A^{(2)}_{(1)}$ and $A^{(g)}_{(1)}$, respectively. We neglect the ground-state depletion (a low-energy excitation condition).

Broad-band pump and probe

If the pump and probe pulses have spectra so broad ($1/\tau \gg |J|, \gamma_0$) that the coherent interaction is available with all exciton levels, then

$$A^{(1)}_{(g)} = \sum_{k'k''} \rho^*_{k'k''}(0)(\vec{d}^{k'}_g\vec{e})(\vec{d}^{k''}_g\vec{e})^*$$

$$A^{(g)}_{(1)} = \sum_{k'k''} \rho_{k'k''}(t)\,(\vec{d}^{g}_{k'}\vec{e})(\vec{d}^{g}_{k''}\vec{e})^* \tag{A1}$$

$$A^{(2)}_{(1)} = \sum_{k'k''}\sum_{k1k2} \rho_{k'k''}(t)(\vec{d}^{k1k2}_{k'}\vec{e})(\vec{d}^{k1k2}_{k''}\vec{e})^*$$

$$\vec{d}^{k}_g = \vec{d}^{g*}_k = \langle k|\hat{d}|g\rangle \qquad \vec{d}^{k1k2}_k = \langle k_2k_1|\hat{d}|k\rangle.$$

The initial conditions are

$$\rho_{k'k''}(0) = \text{const}\,(\vec{d}^{k'}_g\vec{e})(\vec{d}^{k''}_g\vec{e})^*, \tag{A2}$$

where the constant is defined by normalization condition.

If polarization of pump and probe pulses is determined by the vectors $\vec{e}_p$ and $\vec{e}$, respectively, then the difference absorption will be equal to

$$\Delta A(\vec{e}_{p'}, \vec{e}) = A^{(1)}_{(g)}(\vec{e}_p)(A^{(2)}_{(1)}(\vec{e}) - A^{(g)}_{(1)}(\vec{e}) - A^{(1)}_{(g)}(\vec{e})). \tag{A3}$$

For the linear polarized light, $\vec{e}_p = \vec{e}_\parallel$, $\vec{e} = \vec{e}_\parallel, \vec{e}_\perp$, where $\vec{e}_\perp$ is perpendicular to $\vec{e}_\parallel$. The anisotropy degree will be

$$p = \frac{\Delta A(\vec{e}_\parallel, \vec{e}_\parallel) - \Delta A(\vec{e}_\parallel, \vec{e}_\perp)}{\Delta A(\vec{e}_\parallel, \vec{e}_\parallel) + \Delta A(\vec{e}_\parallel, \vec{e}_\perp)} \equiv \frac{\Delta A_\parallel - \Delta A_\perp}{\Delta A_\parallel + \Delta A_\perp}. \tag{A4}$$

Narrow-band pump and probe

If the pump and probe pulses have narrow spectra ($\gamma_0 \ll 1/\tau \ll |J|$), then only the terms ρ_{kk} and $\rho_{k,-k}$ will restored in Eq. A1 and each term in the sum will be multiplied by the function $f(E - (E_{k1k2} - E_k))$ or $f(E - E_k)$. This function represents the overlap of pulse spectrum with transition bands. Here the energy E corresponds to the central frequency of the pulse spectrum and the energies $E_{k1k2} - E_k$ or E_k correspond to the central frequencies of transition bands:

$$A^{(1)}_{(g)}(E) = \sum_k \rho^*_{k,\pm k}(0)(\vec{d}^{k}_g\vec{e})(\vec{d}^{\pm k}_g\vec{e})^* f(E - E_k)$$

$$A^{(g)}_{(1)}(E) = \sum_k \rho_{k,\pm k}(t)(\vec{d}^{g}_k\vec{e})(\vec{d}^{g}_{\pm k}\vec{e})^* f(E - E_k) \tag{A5}$$

$$A^{(2)}_{(1)}(E) = \sum_k\sum_{k1k2} \rho_{k,\pm k}(t)(\vec{d}^{k1k2}_k\vec{e})(\vec{d}^{k1k2}_{\pm k}\vec{e})^* f(E - (E_{k1k2} - E_k)).$$

Initial conditions:

$$\rho_{k'k''}(0) = \text{const}(\vec{d}^{k'}_g\vec{e})(\vec{d}^{k''}_g\vec{e})^* f(E_p - E_k), \tag{A6}$$

where E_p is the energy of exciting quantum. If E is the energy of probing quantum, then instead of Eq. A3 we may write

$$\Delta A(E_p, \vec{e}_p, E, \vec{e}) = A^{(1)}_{(g)}(E_p, \vec{e}_p)\,(A^{(2)}_{(1)}(E, \vec{e}) - A^{(g)}_{(1)}(E, \vec{e}) - A^{(1)}_{(g)}(E, \vec{e})). \tag{A7}$$

APPENDIX B

Expressions for the coefficients in Eqs. 14 and 15 are listed below:

$$
\begin{aligned}
A_{\pm} &= \tfrac{1}{3}(\kappa^2/2 f_p(-2) \pm f_p(1)) \\
&\quad \cdot ((2\kappa^2 \pm \tfrac{4}{3}) f(0) - \kappa^2 f(-2) \pm \tfrac{2}{3} f(3) \pm \tfrac{1}{3} f(-3) \mp f(1)) \\
B_{\pm} &= \kappa^2/2 f_p(-2)\,(\tfrac{4}{3} f(0) - \kappa^2 f(-2) \pm \tfrac{2}{3} f(3)) \\
&\quad + f_p(1)((\tfrac{4}{3} \pm \kappa^2/3) f(0) + \tfrac{1}{3} f(-3) - f(1)) \\
C_{\pm} &= f_p(1)(\tfrac{1}{3} f(-3) - f(1)) \\
D_{\pm} &= (\kappa^2/2 f_p(-2) \pm f_p(1))(\kappa^2 f(-2) \pm 2 f(1)) \\
G &= \tfrac{1}{3}(\tfrac{8}{3} f(0) + \tfrac{2}{3} f(3) + \tfrac{2}{3} f(-3) - 2 f(1)) \\
H &= \tfrac{4}{3} f(0) + \tfrac{1}{3} f(-3) - 2 f(1) \\
E &= \tfrac{1}{3} f(-3) - f(1); \\
I &= 2 f(1).
\end{aligned}
\tag{B1}
$$

Here the functions $f(E - (E_{k1k2} - E_k))$ or $f(E - E_k)$ are denoted $f(\alpha)$, and $f(E_p - E_k)$ as $f_p(\alpha)$, where $\alpha = (E_{k1k2} - E_k - \Delta E)/|M|$ or $\alpha = (E_k - \Delta E)/|M|$.

REFERENCES

Abdourakhmanov, I. A., R. Danielius, A. P. Razjivin, and R. Rotomskis. 1986. The investigation of excited energy relaxation in pigment-protein complex B890 from Chromatium minutissimum by difference picosecond absorption spectroscopy. *In* Poster Abstracts of 7th International Congress on Photosynthesis. Providence, RI. 303-043.

Aslangul, C., and Ph. Kottis. 1974. Density operator description of excitons in molecular aggregates: optical absorption and motion. I. The dimer problem. *Phys. Rev. B.* 10:4364–4382.

Aslangul, C., and Ph. Kottis. 1976. Density operator description of excitons in molecular aggregates. II. Optical line-shape selection rules of "one-dimensional" excitons and excitation localization in finite molecular chains. *Phys. Rev. B.* 13:5544–5559.

Aslangul, C., and Ph. Kottis. 1978. Density operator description of excitons in molecular aggregates. III. Excitonic motion in one-dimensional finite chains. *Phys. Rev. B.* 18:4462–4476.

Bergstrom, H., W. H. J. Westerhuis, V. Sundstrom, R. van Grondelle, R. A. Niederman, and T. Gillbro. 1988. Energy transfer within the isolated B875 light-harvesting pigment-protein complex of *Rhodobacter sphaeroides*: at 77K studied by picosecond absorption spectroscopy. *FEBS Lett.* 233:12–16.

Boonstra, A. F., L. Germeroth, and E. J. Boekma. 1994. Structure of the light harvesting antenna form *Rhodospirillum molischianum* studied by electron microscopy. *Biochim. Biophys. Acta.* 1184:227–234.

Borisov, A. Yu., R. A. Gadonas, R. V. Danielius, A. S. Piskarskas, and A. P. Razjivin. 1982. Minor component B-905 of light-harvesting antenna in Rhodospirillum rubrum chromatophores and the mechanism of singlet-singlet annihilation as studied by difference selective picosecond spectroscopy. *FEBS Lett.* 138:25–28.

Braun, P., and A. Scherz. 1991. Polypeptides and bacteriochlorophyll organization in the light-harvesting complex B850 of *Rhodobacter sphaeroides* R-26.1. *Biochemistry.* 30:5177–5184.

Chesnut, D. B., and A. Suna. 1963. Fermion behavior of one-dimensional excitons. *J. Chem. Phys.* 39:146–149.

Danielius, R., H. Greaner, A. Laubereau, and P. J. M. van Kan. 1992. Vibrational excitation and ultrafast heating of light-harvesting pigments in chromatophores via annihilation and picosecond IR excitation. *In* 4th International Conference on Laser Applications in Life Sciences, Jyvaskyla, Finland. Program and Abstracts. 67.

Danielius, R. V., E. A. Kotova, A. P. Razjivin, R. J. Rotomskis, and V. D. Samuilov. 1986. Dynamics of absorbance changes induced by picosecond light pulses in the light-harvesting complexes from *Rhodospirillum rubrum. Molekularnaya biologiya.* 20:86–91 (In Russian).

Danielius, R. V., V. V. Krasauskas, A. P. Razjivin, and R. J. Rotomskis. 1984. Kinetics of absorption changes of P870 band in chromatophores from *Rhodospirillum rubrum. Biologicheskie Nauki.* 7:34–39 (In Russian).

Danielius, R. V., A. P. Mineyev, and A. P. Razjivin. 1989. The cooperativity phenomena in a pigment-protein complex of light-harvesting antenna revealed by picosecond absorbance difference spectroscopy. *FEBS Lett.* 250:183–186.

Danielius, R., V. Novoderezhkin, and A. Razjivin. 1994. Picosecond absorbance difference spectra of the antenna of photosynthetic purple bacteria: the influence of exciton interactions and librations. *FEBS Lett.* 345:203–206.

Davydov, A. S. 1971. Theory of Molecular Excitons. Plenum Press, New York. 262 pp.

de Boer, S., K. J. Vink, and D. A. Wiersma. 1987. Optical dynamics of condensed molecular aggregates: accumulated photon-echo and hole-burning study of the J-aggregate. *Chem. Phys. Lett.* 137:99–106.

Deinum, G., T. J. Aartsma, R. van Grondelle and J. Amesz. 1989. Singlet-singlet excitation annihilation measurements on the antenna of Rhodospirillum rubrum between 300 and 4K. *Biochim. Biophys. Acta.* 976:63–69.

Drews, G. 1985. Structure and functional organization of light-harvesting complexes and photochemical reaction centers in membranes of phototrophic bacteria. *Microbiol. Rev.* 59–70.

Engelhard, H., W. Baumeister, and W. O. Saxton. 1983. Electron microscopy of photosynthetic membranes containing bacteriochlorophyll b. *Arch. Microbiol.* 135:169–175.

Engelhard, H., A. Engel, and W. Baumeister. 1986. Stoichiometric model of the photosynthetic unit of *Ectothiorhodospira holochloris. Proc. Natl. Acad. Sci. USA.* 83:8972–8976.

Freiberg, A., V. I. Godik, and K. Timpmann. 1984. Excitation energy transfer in bacterial photosynthesis studied by picosecond laser spectroscopy. *In* Advances in Photosynthesis Research, Vol. 1. C. Sybesma, editor. Martinus Nijhoff Publishers. Dordrecht, The Netherlands. 45–48.

Freiberg, A., V. I. Godik, T. Pullerits, and K. Timpmann. 1988. Directed picosecond excitation transport in purple photosynthetic bacteria. *Chem. Phys.* 128:227–235.

Godik, V. I., A. Freiberg, K. Timpmann, A. Yu. Borisov, and K. K. Rebane. 1987. Picosecond excitation energy transfer between different light-harvesting complexes and reaction centers in purple bacteria. *In* Progress in Photosynthesis Research, Vol. 1. Martinus Nijhoff Publishers, Dordrecht, The Netherlands. 41–44.

Godik, V. I., K. Timpmann, A. Freiberg, and A. A. Moskalenko. 1993. Picosecond dynamics of excitations in light-harvesting complex B800–850 from *Chromatium minutissimum* studied using fluorescence spectrochronography. *FEBS Lett.* 327:68–70.

Golubok, A. O., S. A. Vinogradova, S. Y. Tipisev, A. Yu. Borisov, A. S. Taisova, and O. V. Kolomytkin. 1992. STM/STS Study of photosynthetic bacterial membranes. *Ultramicroscopy.* 42–44:1228–1235.

Grad, J., G. Hernander, and S. Mukamel. 1988. Radiative decay and energy transfer in molecular aggregates: the role of intermolecular dephasing. *Phys. Rev. A.* 37:3835–3846.

Haken, H., and G. Strobl. 1967. Exact treatment of coherent and incoherent triplet exciton migration. *In* The Triplet State. A. B. Zahlan, editor. Cambridge University Press, Cambridge. 311–314.

Hunter, C. N., H. Bergstrom, R. van Grondelle, and V. Sundstrom. 1990. Energy transfer dynamics in three light-harvesting mutants of Rhodobacter sphaeroides: a picosecond spectroscopy study. *Biochemistry.* 29:3203–3207.

Juzeliunas, G. 1988. Exciton absorption spectra of optically excited linear molecular aggregates. *Z. Phys. D.* 8:379–384.

Knoester, J. 1993. Nonlinear optical line shapes of disordered molecular aggregates: motional narrowing and the effect of intersite correlations. *J. Chem. Phys.* 99:8466–8479.

Knapp, E. W. 1984. Lineshapes of molecular aggregates. Exchange narrowing and intersite correlation. *J. Chem. Phys.* 85:73–82.

Knox, R. S., and D. Gulen. 1993. Theory of polarized fluorescence from molecular pairs: Forster transfer at large electronic coupling. *Photochem. Photobiol.* 57:40–43.

Knox, R. S., and R. van Metter. 1979. Fluorescence of light-harvesting chlorophyll a/b-protein complexes: implications for the photosynthetic unit. *In*

CIBA Foundation Symp., Vol. 61. Excerpta Medica, New York. 177–186.

Kramer, J. M., J. D. Pennoyer, R. van Grondelle, W. H. J. Westerhuis, R. A. Niederman, and J. Amesz. 1984. Low-temperature optical properties and pigment organization of the B875 light-harvesting bacteriochlorophyll-protein complex of purple photosynthetic bacteria. *Biochim. Biophys. Acta.* 767:335–344.

Lin, S., H. V. Amerongen, and W. S. Struve. 1991. Ultrafast pump-probe spectroscopy of bacteriochlorophyll c antennae in bacteriochlorophyll a-containing chlorosomes from the green photosynthetic bacterium Chloroflexus aurantiacus. *Biochim. Biophys. Acta.* 1060:13–24.

Meckenstock, R. U., K. Krusche, R. A. Brunisholz, and H. Zuber. 1992. The light-harvesting core-complex and the B820-subunit from Rhodopseudomonas marina. II. Electron microscopic characterization. *FEBS Lett.* 311: 135–138.

Miller, K. R. 1982. Three-dimensional structure of a photosynthetic membrane. *Nature.* 300:53–55.

Novoderezhkin, V. I. 1992. Exciton interactions and their influence on picosecond absorbance difference spectra of light-harvesting antenna of purple bacteria. *In* 4th International Conference on Laser Applications in Life Sciences, Jyvaskyla, Finland. Program and Abstracts. 175.

Novoderezhkin, V. I., and A. P. Razjivin. 1993a. Exciton interactions and their influence on picosecond absorbance difference spectra of light-harvesting antenna of purple bacteria. *In* Laser Spectroscopy of Biomolecules. Juoko E. I. Korppi-Tommola, editor. *Proc. SPIE* 1921:102–106.

Novoderezhkin, V. I., and A. P. Razjivin. 1993b. Excitonic interactions in the light-harvesting antenna or photosynthetic purple bacteria and their influence on picosecond absorbance difference spectra. *FEBS Lett.* 330:5–7.

Nuijs, A. M., R. van Grondelle, H. L. P. Joppe, A. C. van Bochove, and L. N. M. Duysens. 1985. Singlet and triplet excited carotenoid and antenna bacteriochlorophyll of the photosynthetic purple bacterium *Rhodospirillum rubrum* as studied by picosecond absorbance difference spectroscopy. *Biochim. Biophys. Acta.* 810:94–105.

Pearlstein, R. M. 1982. Chlorophyll singlet excitons. *In* Photosynthesis: Energy Conversion by Plants and Bacteria, Vol. 1. Govindjee, editor. Academic Press, New York. 293–330.

Pearlstein, R. M., and H. Zuber. 1985. Exciton states and energy transfer in bacterial membranes: the rule of pigment-protein cyclic unit structures. *In* Antennas and reaction centers of photosynthetic bacteria. M. E. Michel-Beyerle, editor. Springer-Verlag, Berlin. 53–61.

Pullerits, T., and A. Freiberg. 1991. Picosecond fluorescence of simple photosynthetic membranes: evidence of spectral inhomogeneity and directed energy transfer. *J. Chem. Phys.* 149:409–418.

Pullerits, T., and A. Freiberg. 1992. Kinetic model of primary energy transfer and trapping in photosynthetic membranes. *Biophys. J.* 63:879–896.

Pullerits, T., K. J. Visscher, S. Hess, V. Sundstrom, A. Freiberg, K. Timpmann, and R. van Grondelle (1994) Energy transfer in the inhomogeneously broadened core antenna of purple bacteria: a simultaneous fit of low-intensity picosecond absorption and fluorescence kinetics. *Biophys. J.* 66:236–248.

Rahman, T. S., R. S. Knox, and V. M. Kenkre. 1979. Theory of depolarization of fluorescence in molecular pairs. *J. Chem. Phys.* 44:197–211.

Razjivin, A. P., R. V. Danielius, R. A. Gadonas, A. Yu. Borisov, and A. S. Piskarskas. 1982. The study of excitation transfer between light-harvesting antenna and reaction center in chromatophores from purple bacterium *Rhodospirillum rubrum* by selective picosecond spectroscopy. *FEBS Lett.* 143:40–44.

Razjivin, A. P., V. I. Sidelnikov, and S. G. Charchenko. 1984. The study of the structure of *Rhodospirillum rubrum* chromatophore absorption spectra by the derivative spectrophotometry. *Studia biophysica.* 102:153–154.

Reddy, N. R. S., G. J. Small, M. Seibert, and R. Picorel. 1991. Energy transfer dynamics of the B800–850 antenna complex of *Rhodobacter sphaeroides*: a hole-burning study. *Chem. Phys. Lett.* 181:391–399.

Reddy, N. R. S., R. Picorel, and G. J. Small. 1992. B896 and B870 components of the Rhodobacter sphaeroides antenna: a hole burning study. *J. Phys. Chem.* 96:6458–6464.

Reddy, N. R. S., R. J. Cogdell, L. Zhao, and G. J. Small. 1993. Nonphotochemical hole burning of the B800–850 antenna complex of Rhodopseudomonas acidophila. *Photochem. Photobiol.* 57:35–39.

Reineker, P. 1982. Stochastic Liouville equation approach: coupled coherent and incoherent motion, optical line shapes, magnetic resonance phenomena. *In* Exciton Dynamics in Molecular Crystals and Aggregates. Springer tracts in modern physics, Vol. 94. Springer-Verlag, Berlin. 111–226.

Sebban, P., G. Jolchine, and I. Moya. 1984. Spectra of fluorescence lifetime and intensity of *Rhodopseudomonas sphaeroides* at room and low temperature. Comparison between the wild type, the C-71 reaction center-less mutant and the B800–850 pigment-protein complex. *Photochem. Photobiol.* 39:247–253.

Sebban, P., and I. Moya. 1983. Fluorescence lifetime spectra of in vivo bacteriochlorophyll at room temperature. *Biochim. Biophys. Acta.* 722:436–442.

Shepanski, J. F., and R. S. Knox. 1981. Circular Dichroism and other Optical Properties of antenna chlorophyll proteins from Higher Plants. *Isr. J. Chem.* 21:325–331.

Somsen, O. J. G., F. van Mourik, R. van Grondelle, and L. Valkunas. 1993. Energy migration and trapping in a spectrally and spatially inhomogeneous light-harvesting antenna. *Biophys. J.* 66:1580–1596.

Spano, F. C., J. R. Kuklinski, and S. Mukamel. 1990. Temperature-dependent superradiant decay of excitons in small aggregates. *Phys. Rev. Lett.* 65:211–214.

Sundstrom, V., R. van Grondelle, H. Bergstrom, E. Akesson, and T. Gillbro. 1986. Excitation energy transport in the bacteriochlorophyll antenna systems of *Rhodospirillum rubrum* and *Rhodobacter sphaeroides*, studied by low-intensity picosecond absorption spectroscopy. *Biochim. Biophys. Acta.* 851:431–446.

Thornber, J. P., R. J. Cogdel, B. K. Pierson, and R. E. B. Seftor. 1983. Pigment-protein complexes of purple photosynthetic bacteria: an overview. *J. Cell. Biochem.* 23:159–169.

Timpmann, K., A. Freiberg, and V. I. Godik. 1991. Picosecond kinetics of light excitations in photosynthetic purple bacteria in the temperature range of 300–4K. *Chem. Phys. Lett.* 182:617–622.

Valkunas, L., A. Razjivin, and G. Trinkunas. 1985. Interaction of the minor spectral form bacteriochlorophyll with antenna and the reaction centre in the process of excitation energy transfer in photosynthesis. *Photobiochem. Photobiophys.* 9:139–142.

van Grondelle, R., H. Bergstrom, V. Sundstrom, and T. Gillbro. 1987. Energy transfer within the bacteriochlorophyll antenna of purple bacteria at 77K, studied by picosecond absorption recovery. *Biochim. Biophys. Acta.* 894:313–326.

van Grondelle, R., H. Bergstrom, V. Sundstrom, R. J. van Dorssen, M. Vos, and C. N. Hunter. 1988. Excitation energy transfer in the light-harvesting antenna of photosynthetic purple bacteria: the rule of the long-wavelength absorbing pigment B896. *In* Photosynthetic light-harvesting systems. H. Scheer and S. Schneider, editors. Walter de Gruyter & Co., New York. 519–530.

van Grondelle, R., F. van Mourik, R. W. Visschers, O. J. G. Somsen, and L. Valkunas. 1992. The bacterial photosynthetic light-harvesting antenna aggregation state, spectroscopy and excitation energy transfer. *In* Research in Photosynthesis, Vol. 1. Kluwer Academic Publishers, The Netherlands. 9–16.

van Metter, R. L. 1977. Excitation energy transfer in the light-harvesting chlorophyll a/b protein. *Biochim. Biophys. Acta.* 462:642–658.

van Mourik, F., R. W. Visschers, and R. van Grondelle. 1993. Spectral inhomogeneity of the light-harvesting antenna of *Rhodospirillum rubrum* probed by triplet-minus-singlet spectroscopy and singlet-triplet annihilation at low temperatures. *Photochem. Photobiol.* 57:19–23.

Visschers, R. W., F. van Mourik, R. Monshouwer, and R. van Grondelle. 1993. Inhomogeneous spectral broadening of the B820 subunit from LH1. *Biochim. Biophys. Acta.* 1141:238–244.

Vos, M., R. van Grondelle, F. W. van der Kooij, D. van der Poll, J. Amesz, and L. N. M. Duysens. 1986. Singlet-singlet annihilation at low temperatures in the antenna of purple bacteria. *Biochim. Biophys. Acta.* 850: 501–512.

Zuber, H. 1985. Structure and function of light-harvesting complexes and their polypeptides. *Photochem. Photobiol.* 42:821–844.

Zuber, H., and R. N. Brunisholz. 1991. Structure and function of antenna polypeptides and chlorophyll protein complexes: principles and variability. *In* Chlorophylls. H. Scheer, editor. CRC Press, Boca Raton, FL. 627–703.

Zuber, H., R. Brunisholz, and W. Sidler. 1987. Structure and function of light-harvesting pigment-protein complexes. *In* Photosynthesis (New Comprehensive Biochemistry, Vol. 15). J. Amesz, editor. Elsevier Scientific Publishers B. V. (Biomedical Division), New York. 233–271.